Magnetization density in Ce_3Al_{11}

1995 J. Phys.: Condens. Matter 7 8821

(http://iopscience.iop.org/0953-8984/7/46/012)

J. Phys.: Condens. Matter 7 (1995) 8821–8831. Printed in the UK

Magnetization density in Ce_3Al_{11}

A Muñoz†§, F Batallan‡, J X Boucherle†‖, F Givord†‖, G Lapertot†, E Ressouche† and J Schweizer†

† Commissariat à l'Energie Atomique, Département de Recherche Fondamentale sur la Matière Condensée, SPSMS/MDN, Centre d'Etudes Nucléaires de Grenoble, 17 rue des Martyrs, 38054 Grenoble Cédex 9, France

‡ Instituto de Ciencia de Materiales, Consejo Superior de Investigaciones Cientificas, Madrid, Spain

Received 13 June 1995

Abstract. Ce_3Al_{11} is an orthorhombic compound in which the cerium atoms occupy two different sites. Due to the crystal structure, the presence of twins cannot be avoided. Kondo effects are present, leading to unusual magnetic properties. Below the ordering temperature, 6.2 K, neutron diffraction experiments performed on powder, and more recently on single crystals, evidenced two different magnetic phases: the compound is ferromagnetic between 6.2 K and 3.2 K, and becomes modulated with an incommensurate propagation vector $k = (0, 0, kz)$ at lower temperatures. In both phases, the cerium moments are very different on the two sites, one of them being strongly reduced. However, from the integrated magnetic intensities alone, one cannot determine on which of the two sites the moment is reduced.

Polarized neutron measurements were undertaken to remove this ambiguity and to obtain the magnetization density maps. The easy magnetization direction being along the b-direction, the experiment was performed with b parallel to the applied field. However, in the projection onto the plane perpendicular to b, the two cerium sites are superimposed and cannot be separated. It was then necessary to measure the magnetic density in three dimensions. To overcome the twin problem, measurements were performed for two orientations of the crystal and a new procedure for data treatment was used. The magnetization density maps obtained from Fourier inversion or by the three-dimensional maximum entropy method clearly show that the reduced cerium moment is on the less symmetric crystallographic site.

1. Introduction

Ce_3Al_{11} is one of the cerium–aluminium compounds in which a coexistence of Kondo effects and magnetic interactions is observed. Kondo-type behaviour was deduced from the presence of a minimum in the electrical resistivity at high temperatures [1] and from the rather large value of the γ coefficient in the specific heat ($\gamma = 100$ mJ K^{-2} for Ce_3Al_{11}) [2]. At low temperatures, magnetic interactions dominate and magnetic orderings of the moments of the two Ce sites take place below 6.2 K [3].

Recently, we have succeeded in growing large single crystals and we have confirmed, by neutron diffraction, the unusual transition from a ferromagnetic phase to a modulated structure as the temperature is decreased. In the temperature range 3.2 K $< T <$ 6.2 K the structure is ferromagnetic with all the Ce magnetic moments parallel to the b axis. Below

§ Present address: Escuela Politecnica Superior, Departamento de Ingenieria, Area de Fisica Aplicada, Calle Butarque 15, 28911 Leganes, Madrid, Spain.

‖ Centre National de la Recherche Scientifique staff.

0953-8984/95/468821+11$19.50

$T = 3.2$ K a modulated structure was found, with a propagation vector $k = (0, 0, \sim \frac{1}{3})$ and moments also parallel to b. In the two phases, the cerium moments are very different on the two sites: one has an almost normal value, whereas the other is strongly reduced. However, from the integrated magnetic intensities alone, one cannot determine on which of the two sites the moment is reduced.

Polarized neutron measurements were undertaken to obtain the magnetization density maps and to remove this ambiguity.

2. Experimental details

2.1. Sample characterization

Ce_3Al_{11} crystallizes into the orthorhombic La_3Al_{11} structure [4] with space group $Immm$. The parameters are:

$$a = 4.395 \text{ Å} \qquad b = 13.025 \text{ Å} \qquad c = 10.092 \text{ Å}.$$

Note that a and b satisfy the relation $b \sim 3a$. The correlation between these parameters comes from the fact that the Ce_3Al_{11} structure is deduced from the tetragonal structure of $BaAl_4$ by ordered substitutions of atoms every third cell. The cerium skeleton structure can almost be described by a stacking along b of three tetragonal cells $(a, b/3 \sim a, c)$. Consequently, there are two different sites for Ce atoms, one (Ce_I) with an mmm symmetry (2a) in position $(0, 0, 0)$ and one (Ce_{II}) with a lower $m2m$ symmetry (4g) in position $(0, -y, 0)$ and a value of y close to $\frac{1}{3}$. For the same reason, it is impossible to obtain single crystals without twins.

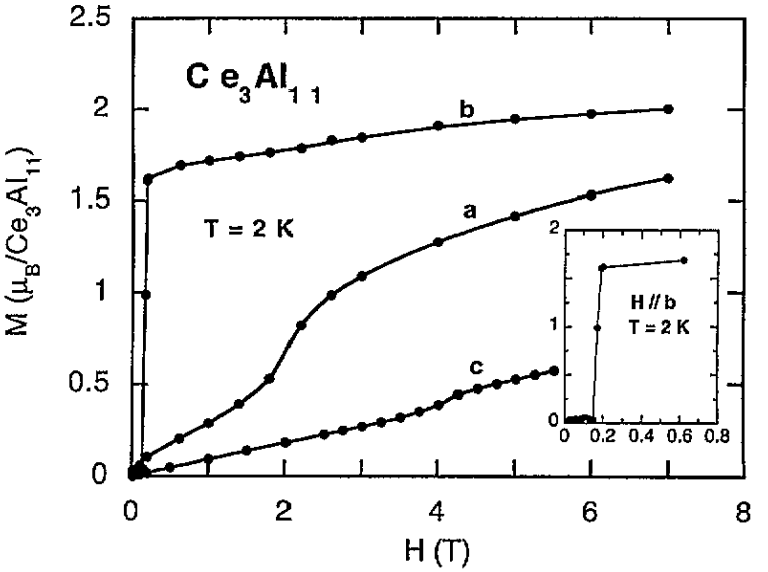

Figure 1. Isothermal magnetization curves at $T = 2$ K in a Ce_3Al_{11} single crystal along the a, b and c axes. Inset: detail in the low-field region of the induced magnetic transition along the b axis. The lines are guides for the eye.

A 5 mm^3 single crystal [3] was used for the measurements. The domain proportion (82.6%/17.4%) was determined from a structure refinement using results of measurements on a 4-circle neutron diffractometer [3].

Magnetization was previously measured [3] along the principal crystallographic directions on this single crystal (figure 1).

2.2. *Polarized neutron experiments*

Polarized neutron diffraction experiments were performed on the DN2 spectrometer (Siloé reactor, CEN-Grenoble). This is a two-axis spectrometer with lifting counter, equipped with a cryomagnet system producing magnetic fields up to 4.6 T in the vertical direction. The wavelength is $\lambda = 1.2$ Å. For this type of measurement all the moments have to be parallel to the polarization direction, that is the vertical magnetic field.

As the easy magnetization direction is along the b-direction, a first experiment was performed at 2 K with b vertical for the biggest partner $x = 82.6\%$ of the crystal. Due to the presence of twins, the smallest partner $y = 17.4\%$ of the crystal is then oriented with a vertical. Previous magnetic structure determinations at this temperature have shown [3] that, with such a field ($H = 4.6$ T) applied along b and a, the modulated structures are changed into ferromagnetic-type structures with all the moments parallel to the field.

As well as reflections characteristic of the main partner ($x = 82.6\%$) of the twin only, there are other reflections for which both partners of the twin will give contributions at the same Bragg positions. This can be seen on the scheme of the reciprocal lattices for the two orientations b and a vertical (figure 2). These reflections are:

$(h, k = 3n, l)$, b vertical for crystal x;

with magnetic structure factor $xF_M(h, k = 3n, l) = xF_{Mb}$

$(k/3 = n, 3h, l)$, a vertical for crystal y;

with magnetic structure factor $yF_M(k/3 = n, 3h, l) = yF'_{Ma}$.

This is especially the case for all the reflections measured in the equatorial plane $(h, 0, l)$.

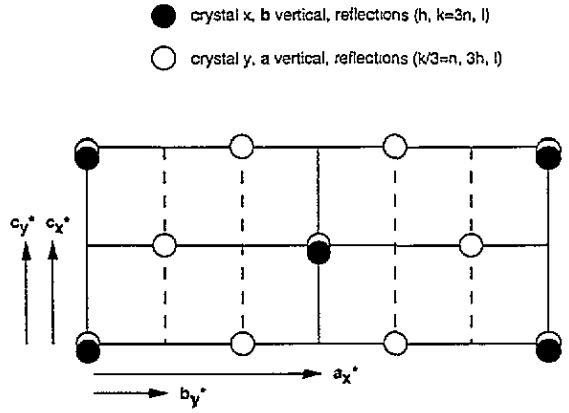

Figure 2. Horizontal planes containing reflections from the two partners of the twin in the reciprocal lattice: the crystal x is orientated with b vertical and the crystal y with a vertical.

Usually, from flipping ratios R measured with polarized neutrons, it is possible to directly obtain the magnetic structure factor, knowing the nuclear one. In this first experiment, there are two terms to determine from the flipping ratios R_1 of these reflections: F_{Mb} and F'_{Ma}. A second experiment was then performed with a vertical for $x = 82.6\%$

of the crystal, and therefore b vertical for $y = 17.4\%$. This gave the flipping ratio R_2 involving yF_{Mb} and xF'_{Ma}.

In a polarized neutron diffraction experiment with b vertical, the more commonly measured reflections are the $(h, 0, l)$ ones and they lead to a projection on the plane perpendicular to b on the magnetization density maps. Unfortunately, in such a projection, the two cerium sites are superimposed and cannot be separated. It was therefore also necessary to measure reflections of type (h, k, l) with $k = 1, 2, 3$ and 4 in order to get the magnetic density of the whole space. For the first experiment, 187 flipping ratios R_1 were measured corresponding to 110 independent (h, k, l) reflections. For the second experiment, 121 flipping ratios R_2 were measured corresponding to 68 independent $(0, k, l)$ and $(1, k, l)$ reflections. The experimental conditions are summarized in table 1.

Table 1. Experimental conditions for measurements of flipping ratios.

	$\lambda = 1.2$ Å $C_{\lambda/2} = \frac{1}{8}J(\lambda/2)/J(\lambda) = 0.0027$ $p = -0.934$ $e = 1.0$ $H = 4.6$ T $T = 2$ K			
	1st experiment $H \parallel b$ for $x = 82.6\%$ $H \parallel a$ for $y = 17.4\%$		2nd experiment $H \parallel a$ for $x = 82.6\%$ $H \parallel b$ for $y = 17.4\%$	
Contribution	x	$x + y$	y	$x + y$
Number of measured reflections	$(h, 1, l)$ 40 $(h, 2, l)$ 32 $(h, 4, l)$ 35	$(h, 0, l)$ 46 $(h, 3, l)$ 34	$(0, k, l)$ 16 $(1, k, l)$ 17 $(k \neq 3n)$	$(0, k, l)$ 50 $(1, k, l)$ 38 $(k = 3n)$
Total	187		121	
Number of independant reflections	$(h, 1, l)$ 22 $(h, 2, l)$ 20 $(h, 4, l)$ 21	$(h, 0, l)$ 27 $(h, 3, l)$ 20	$(0, k, l)$ 12 $(1, k, l)$ 9 $(k \neq 3n)$	$(0, k, l)$ 27 $(1, k, l)$ 20 $(k = 3n)$
Total	110		68	

3. Results and discussion

3.1. Flipping ratios for the case of twinned crystals

For each of the two experiments, there are two types of reflections, due to the contribution of one partner only or of the two partners of the twin. In the first experiment (b vertical for $x = 82.6\%$ of the crystal), reflections of type $(h, k \neq 3n, l)$ correspond to those involving the main partner only. Their flipping ratios are expressed in the classical way:

$$R = \frac{I^+}{I^-} = \frac{F_N^2 + 2pq^2 F_N F_M + q^2 F_M^2 + L^+_{\lambda/2}}{F_N^2 - 2epq^2 F_N F_M + q^2 F_M^2 + L^-_{\lambda/2}}$$

where p is the beam polarization, e the flipping efficiency and $q = \sin\alpha$, α being the angle between the scattering vector Q and the moment direction. $L_{\lambda/2}$ is the $\lambda/2$ contamination correction. All the values used for the corrections are gathered in table 1. The nuclear structure factors F_N are calculated from the structure refinement [3] performed on the same crystal at room temperature. Extinction corrections can be neglected. The magnetic structure factors F_M are obtained by solving a second-order equation with the usual programmes.

In contrast, the intensities of the reflections of type $(h, k = 3n, l)$ are mixed with those of reflections of type $(n, 3h, l)$ from the other partner of the twin (figure 2). The flipping ratios R_1 and R_2 for the first and second experiments depend on the magnetic structure factors of both reflections. A new procedure for the data treatment is necessary in order to separate the two contributions: one gets a fourth-order equation to solve, in order to obtain the magnetic structure factors of the main partner. The details of the calculation are given in the appendix. The data and the magnetic structure factors of the equatorial layer, deduced for the main partner with the b direction vertical, are presented in table 2.

3.2. Magnetization density

3.2.1. Principles. The magnetic structure factors provided by the polarized neutron diffraction experiments are the Fourier components of the magnetization density $m(xyz)$. To obtain this density, one has to solve the inverse Fourier problem. The procedure is complicated by the presence of noise and the incompleteness of the data. For this reason, an infinity of maps can agree with the collected data, and one has to choose the best map from all of the possible ones.

The most straightforward approach is the Fourier inversion. This technique has been widely used in this field but it presents severe drawbacks: (i) error bars are not taken into account, (ii) the non-measured Fourier components are artificially set to zero. These two points introduce artefacts in the reconstruction.

The application of the maximum entropy principle was a breakthrough in this field. The method consists of applying a choice criterion to select from all the possible maps the one which has the highest intrinsic probability, that is the one that maximizes the Boltzmann entropy

$$S(xyz) = -\int_{\text{unitcell}} s(xyz)\ln[s(xyz)]\,dx\,dy\,dz$$

with

$$s(xyz) = m(xyz) \Big/ \int_{\text{unitcell}} m(xyz)\,dx\,dy\,dz.$$

This formula strictly applies for positive densities, but the calculation has been modified by Papoular to treat possible negative densities [5].

In the reconstruction of a magnetization density projection onto a particular plane, the Fourier inversion method makes use of the structure factors measured in the projection plane only. All the other components contribute nothing to the projected density. In contrast, it has been shown that the maximum entropy method may take advantage of all the three-dimensional data collected to yield better quality reconstructed two-dimensional projected maps [6, 7].

Both methods have been used for Ce_3Al_{11} and the results are compared below.

3.2.2. Results from Fourier transformations. The map of the projection onto the (a, c) plane calculated by Fourier transformation is presented in figure 3 (top). The magnetic density is concentrated on the position of the Ce atoms, the fluctuations outside being insignificant, and the shape of the density looks quite cylindrical. However, on this projection the two types of Ce atoms are located in the same place, and it is not possible to distinguish between the two sites. Projections in the other directions are necessary.

The magnetization densities obtained for the two projections along a (left) and along c (right) are presented in figure 3 (bottom). These maps show very clearly that the moments

Table 2. Nuclear structure factors and measured flipping ratios for the layer $k = 0$. Deduced magnetic structure factors F_{Mb}.

				1st experiment					2nd experiment				
h	$3n$	l	F_N	R_1	DR_1	n	$3h$	l	F'_N	R_2	DR_2	F_{Mb}	DF_{Mb}
2	0	0	10.282 62	0.733 362	0.001 529	0	6	0	8.470 61	0.782 904	0.002 471	3.288 828	0.148 452
4	0	0	9.747 77	0.801 695	0.007 282	0	12	0	4.512 54	0.811 327	0.008 255	2.145 265	0.115 798
1	0	1	0.208 18	0.493 543	0.009 920	0	3	1	0.271 91	0.301 176	0.009 181	4.443 016	0.349 265
0	0	2	−0.482 93	5.003 098	0.072 718	0	0	2	−0.482 93	3.285 511	0.055 841	4.005 453	0.185 252
1	0	3	4.625 57	0.452 472	0.003 733	0	3	3	4.037 9 6	0.563 819	0.007 910	3.819 016	0.087 073
3	0	3	4.495 31	0.575 021	0.005 655	0	9	3	4.345 43	0.718 873	0.022 403	2.703 554	0.086 924
5	0	3	4.246 99	0.689 286	0.019 324	0	15	3	3.952 99	0.853 722	0.025 548	1.774 548	0.132 665
0	0	4	3.915 31	0.414 429	0.002 309	0	0	4	3.915 31	0.501 736	0.002 535	3.605 847	0.086 274
2	0	4	3.864 19	0.436 676	0.004 429	0	6	4	2.347 99	0.456 806	0.010 545	3.186 435	0.104 995
4	0	4	3.715 29	0.556 795	0.014 471	0	12	4	−0.694 27	0.548 894	0.036 063	2.151 987	0.202 308
1	0	5	3.091 39	0.397 717	0.010 580	0	3	5	3.985 24	0.573 942	0.013 261	3.269 685	0.168 329
3	0	5	3.022 94	0.419 007	0.013 477	0	9	5	1.611 57	0.431 771	0.020 708	2.594 985	0.164 596
5	0	5	2.890 81	0.492 179	0.041 429	0	15	5	−0.809 17	0.517 997	0.067 404	2.028 617	0.608 585
0	0	6	2.115 20	0.254 972	0.007 370	0	0	6	2.115 20	0.354 521	0.006 780	2.985 360	0.164 220
2	0	6	2.100 69	0.312 503	0.010 796	0	6	6	2.638 50	0.551 477	0.037 653	2.865 403	0.157 634
4	0	6	2.057 19	0.555 872	0.058 741	0	12	6	3.263 47	0.807 680	0.051 550	1.654 175	0.209 704
0	0	8	6.536 74	0.674 198	0.005 945	0	0	8	6.536 74	0.728 338	0.005 760	2.678 516	0.106 292
2	0	8	6.431 22	0.701 556	0.006 014	0	6	8	5.611 90	0.765 026	0.012 723	2.370 230	0.103 101
4	0	8	6.125 74	0.779 274	0.012 763	0	12	8	3.616 88	0.790 371	0.020 351	1.521 395	0.143 961
0	0	10	3.196 54	0.517 301	0.020 666	0	0	10	3.196 54	0.611 260	0.022 816	2.214 147	0.235 374
2	0	10	3.158 98	0.544 604	0.026 713	0	6	10	2.915 58	0.658 241	0.044 888	2.029 227	0.184 189
4	0	10	3.049 16	0.678 573	0.048 558	0	12	10	2.128 75	0.663 085	0.080 967	1.157 248	0.213 950
1	0	11	6.022 12	0.722 030	0.010 383	0	3	11	2.908 64	0.670 701	0.028 557	1.899 946	0.129 722
3	0	11	5.832 15	0.779 635	0.012 891	0	9	11	4.388 20	0.799 351	0.023 343	1.462 280	0.155 475

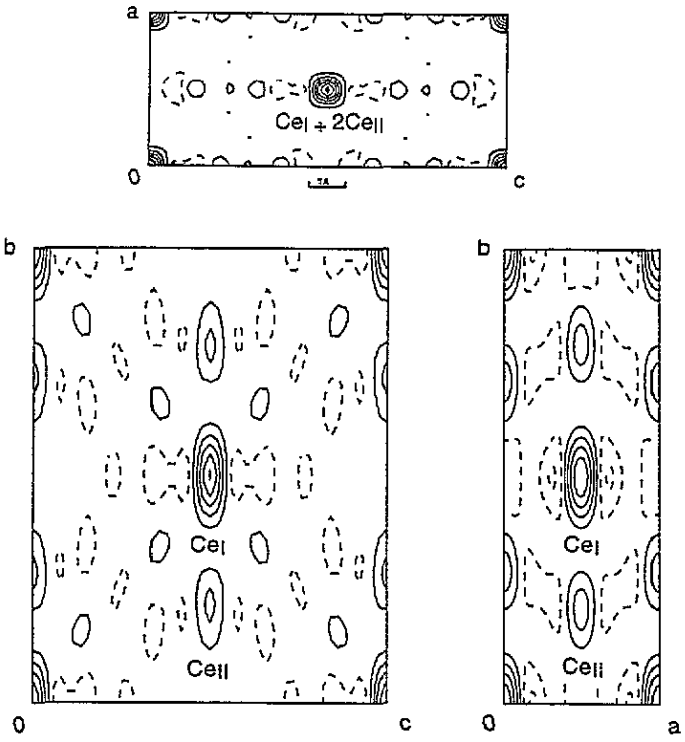

Figure 3. Projection onto the (a, c) (top), (b, c) (bottom left) and (a, b) (bottom right) planes of the magnetization density in Ce_3Al_{11}, calculated by Fourier transformation. The steps between the contour lines are 0.8 μ_B Å^{-2} for the top map and 0.2 μ_B Å^{-2} for the bottom maps.

on the two Ce sites are different, the one in (000) (Ce_I) being about twice as large as the other (Ce_{II}) . The densities have an elongated shape around the atomic sites. This can be explained partly by the poor resolution along the b direction: the maximum value of $\sin\theta/\lambda$ is 0.19 Å^{-1} only, whereas it is 0.57 Å^{-1} perpendicular to b. It can also be partly due to the shape of the magnetic cloud aroud the cerium atoms.

3.2.3. Results from maximum entropy calculations. In figure 4 the magnetization densities obtained by three-dimensional maximum entropy calculations and projected along a (left) and c (right) are shown. These maps confirm the results obtained from the Fourier maps: the two Ce are different, the one on the more symmetric crystallographic site being the more magnetic. Some anisotropy of the shape is also observed. To check whether this anisotropy is not an artefact of the data treatment, the densities projected along a obtained using the two methods (Fourier transformation and maximum entropy calculations) are compared in figure 5. The three drawings, performed for a quarter of the cell, correspond to: (left) Fourier transformation of the data, (middle) maximum entropy calculation of the data, (right) maximum entropy calculation of the structure factors obtained, for the same reflections and with the same experimental errors, in the case of a spherical density.

In the case of spherical density, some anisotropy remains, due to the very large differences in resolution along the two directions. In the experimental maximum entropy map, the extra anisotropy, compared to the previous case represents the real anisotropy. For the Fourier case, the effects due to the poor resolution are drastic.

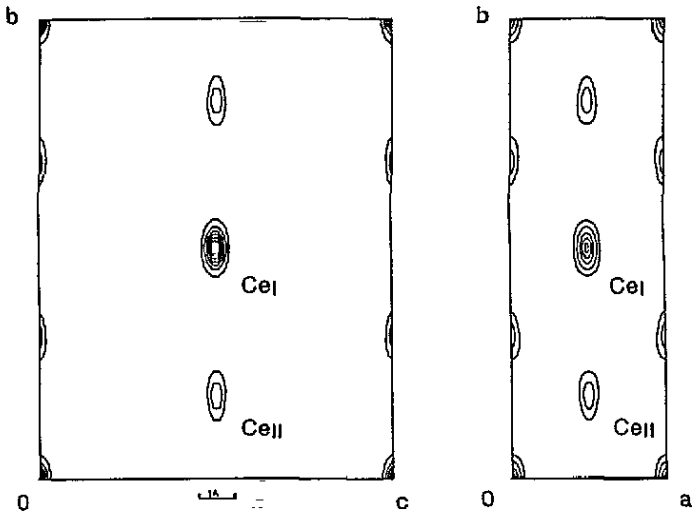

Figure 4. Projections on the (b, c) (left) and (a, b) (right) planes of the magnetization density in Ce_3Al_{11}, deduced from three-dimensional maximum entropy calculations. The steps between the contour lines are 0.8 μ_B Å^{-2}.

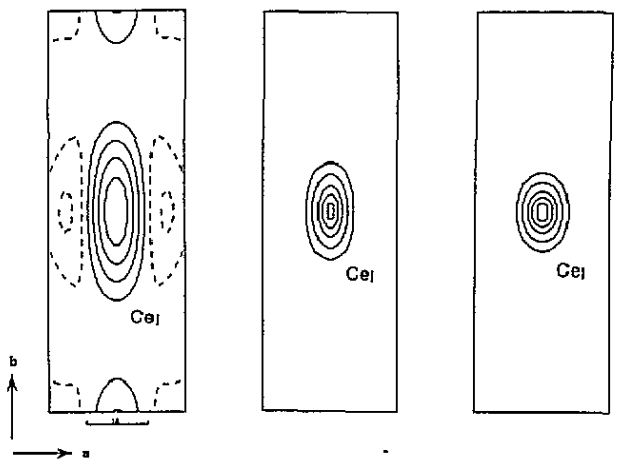

Figure 5. Comparison of the projections on the (a, b) plane of the magnetization density in Ce_3Al_{11}, calculated by Fourier transformation (left) and deduced from three-dimensional maximum entropy calculations in the experimental case (middle) and for a spherical density (right). Only a quarter of the cell is represented.

3.3. Magnetic form factor

As long as the shape of the magnetization density on the two Ce atoms is the same, it is possible to calculate the magnetic form factor in the horizontal (a, c) plane. The magnetic structure factors in this plane correspond to the sum of three moments, one on the Ce_I site and two on the Ce_{II} site. Considering that there is virtually no anisotropy in this plane (figure 3), four different calculations were performed, where the only parameter was the value of the sum of the three moments: the magnetization density is either isotropic (dipolar approximation) or presents an axial symmetry along b, i.e. the wavefunction is a pure $|\frac{5}{2}, m\rangle$

state. Previous calculations [8] show that the extention in the basal plane is rather different for the three possible levels $|\frac{5}{2}, \frac{5}{2}\rangle$, $|\frac{5}{2}, \frac{3}{2}\rangle$, $|\frac{5}{2}, \frac{1}{2}\rangle$.

The four calculations are compared with the experimental points in figure 6. The best agreement corresponds to the $|\frac{5}{2}, \frac{3}{2}\rangle$ calculation. This level leads to a theoretical moment of $\frac{3}{2} g_J \mu_B = 1.29 \mu_B$, a value very close to that of $1.2 \pm (0.10) \mu_B$ obtained for the Ce_I moment at low temperatures and under an applied field [3]. Moreover, the magnetization density of such a level [8] is slightly elongated along the quantification axis, that is the field axis *b*. It corresponds rather well to the anisotropy observed in the maximum entropy maps.

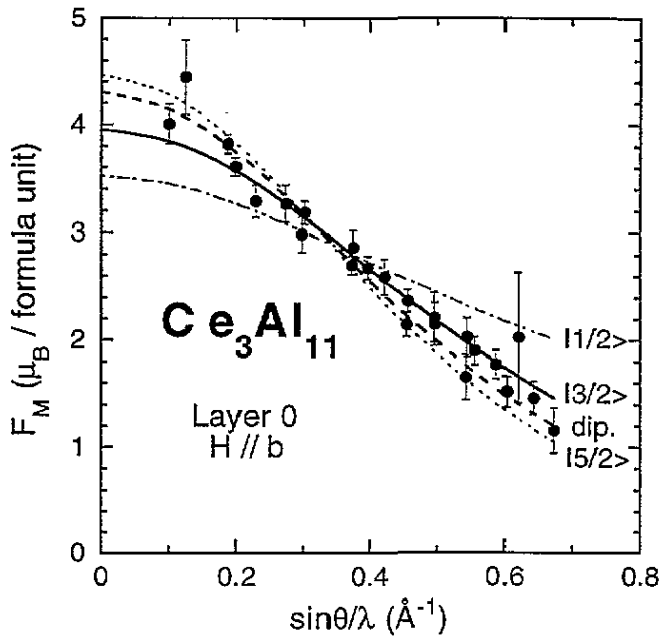

Figure 6. Magnetic structure factors of the equatorial plane (dark circles). Comparison of four calculations. (i) dipolar approximation (dotted line, large dash), (ii) $|\frac{5}{2}, \frac{5}{2}\rangle$ wavefunction (dotted line, small dash), (iii) $|\frac{5}{2}, \frac{3}{2}\rangle$ wavefunction (continuous line), (iv) $|\frac{5}{2}, \frac{1}{2}\rangle$ wavefunction (chain curve).

4. Conclusion

We have shown that it is possible to determine a magnetization density on a twinned crystal, using polarized neutron diffraction. The results evidence without ambiguity that the moments on the two cerium sites have quite different values: the moment on the less symmetric crystallographic site Ce_{II} is strongly reduced.

The analyses of the shape of the magnetization density from both maximum entropy maps and magnetic form factors reveals that the ground-state wavefunction can be of $|\frac{5}{2}, \frac{3}{2}\rangle$ type. As the shape of the densities is very similar for the two cerium atoms, the reduction of the Ce_{II} moment is not due to crystal field effects and the Kondo effect must be put forward.

Appendix

In the first experiment, one measures:

(i) the reflections $(h, k = 3n, l)$ for $x\%$ of the crystal with b vertical: $F_N(h, 3n, l) = F_N$ and $F_M(h, 3n, l) = F_{Mb}$

(ii) the reflections $(k/3 = n, 3h, l)$ for $y\%$ of the crystal with a vertical: $F_N(n, 3h, l) = F'_N$ and $F_M(n, 3h, l) = F'_{Ma}$.

In the second experiment, one measures:

(iii) the reflections $(n, 3h, l)$ for $x\%$ of the crystal with a vertical (F'_N and F'_{Ma})

(iv) the reflections $(h, 3n, l)$ for $y\%$ of the crystal with b vertical (F_N and F_{Mb}).

The flipping ratios R_1 and R_2 for the two experiments are then:

$$R_1 = \frac{xI_b^+(h, 3n, l) + yI_a^+(n, 3h, l) + L_{1\lambda/2}}{xI_b^-(h, 3n, l) + yI_a^-(n, 3h, l) + L_{1\lambda/2}}$$

$$R_2 = \frac{xI_a^+(n, 3h, l) + yI_b^+(h, 3n, l) + L_{2\lambda/2}}{xI_a^-(n, 3h, l) + yI_b^-(h, 3n, l) + L_{2\lambda/2}}$$

with

$$I_b^+(h, 3n, l) = F_N^2 + 2pq^2 F_N F_{Mb} + q^2 F_{Mb}^2$$
$$I_b^-(h, 3n, l) = F_N^2 - 2epq^2 F_N F_{Mb} + q^2 F_{Mb}^2$$
$$I_a^+(n, 3h, l) = F_N'^2 + 2pq^2 F'_N F'_{Ma} + q^2 F_{Ma}'^2$$
$$I_a^-(n, 3h, l) = F_N'^2 - 2epq^2 F'_N F'_{Ma} + q^2 F_{Ma}'^2$$

q^2 will have the value q_1^2 or q_2^2 depending on the experiment it refers to. $L_{1\lambda/2}$ and $L_{2\lambda/2}$ are the $\lambda/2$ corrections on the nuclear structure factors for each experiment:

$$L_{1\lambda/2} = C_{\lambda/2}\left(x|F_N(2h, 6n, 2l)|^2 + y|F'_N(2n, 6h, 2l)|^2\right)$$
$$L_{2\lambda/2} = C_{\lambda/2}\left(x|F'_N(2n, 6h, 2l)|^2 + y|F_N(2h, 6n, 2l)|^2\right).$$

If as usual: $\gamma = F_{Mb}/F_N$ and $\gamma' = F'_{Ma}/F'_N$, the expressions for R_1 and R_2 lead to two second-order equations in γ and γ':

$$A_1\gamma^2 + A'_1\gamma'^2 + B_1\gamma + B'_1\gamma' + C_1 = 0 \qquad \text{(A1)}$$
$$A_2\gamma^2 + A'_2\gamma'^2 + B_2\gamma + B'_2\gamma' + C_2 = 0 \qquad \text{(A2)}$$

with:

$$A_1 = x(1 - R_1)q_1^2 F_N^2 \qquad A'_1 = y(1 - R_1)q_1^2 F_N'^2$$
$$B_1 = 2xp(1 + eR_1)q_1^2 F_N^2 \qquad B'_1 = 2yp(1 + eR_1)q_1^2 F_N'^2$$
$$C_1 = (1 - R_1)[xF_N^2 + yF_N'^2 + L_{1\lambda/2}]$$
$$A_2 = y(1 - R_2)q_2^2 F_N^2 \qquad A'_2 = x(1 - R_2)q_2^2 F_N'^2$$
$$B_2 = 2yp(1 + eR_2)q_2^2 F_N^2 \qquad B'_2 = 2xp(1 + eR_2)q_2^2 F_N'^2$$
$$C_2 = (1 - R_2)[yF_N^2 + xF_N'^2 + L_{2\lambda/2}].$$

The combination of equations (1) and (2) leads to a fourth-order equation in γ:

$$a_4\gamma^4 + a_3\gamma^3 + a_2\gamma^2 + a_1\gamma + a_0 = 0 \qquad \text{(A3)}$$

where the coefficients a_i are expressed as a function of $A_{1(2)}$, $A'_{1(2)}$, $B_{1(2)}$, $B'_{1(2)}$ and $C_{1(2)}$. For each pair of measured flipping ratios R_1 and R_2, the coefficients a_i are calculated. Equation

(A3) was solved by using a subroutine which uses the Laguerre method to calculate the solutions of an nth degree polynomial [9]. Physical considerations helped us to choose between the four possible solutions.

References

[1] Van Daal H J and Buschow K H J 1970 *Phys. Lett.* **31A** 103
[2] Berton A, Chaussy J, Cornut B, Lasjaunias J L, Odin J and Peyrard J 1980 *J. Magn. Magn. Mater.* **15–18** 379
[3] Boucherle J X, Givord F, Lapertot G, Muñoz A and Schweizer J 1995 *J. Magn. Magn. Mater.* **140–144** 1229
[4] Buschow K H J and Van Vucht J H N 1967 *Philips. Res. Rep.* **22** 233
[5] Papoular R J and Gillon B 1990 *Europhys. lett.* **13** 429
[6] Papoular R J, Ressouche E, Schweizer J and Zheludev A 1993 *Maximum Entropy and Bayesian Methods* ed A Mohammad-Djafari and G Demoments (Dordrecht: Kluwer Academic) p 311
[7] Papoular R J, Zheludev A, Ressouche E and Schweizer J 1995 *Acta Crystallogr.* A **51** 295
[8] Boucherle J X, Givord D and Schweizer J 1982 *J. Physique Coll.* **C7** 199
[9] Press H W, Flannery P B, Teukolsky A S and Vetterling T W 1986 *Numerical Recipes, The Art of Scientific Computing* (Cambridge: Cambridge University Press)